Electromechanical actuation of CNT/PVDF composite films based on a bridge configuration*

Xiaogang Gu(谷孝刚)[1,2,3], Xiaogang Xia(夏小刚)[1,2,3], Nan Zhang(张楠)[1,3], Zhuojian Xiao(肖卓建)[1,2,3], Qingxia Fan(范庆霞)[1,3], Feng Yang(杨丰)[1,2,3], Shiqi Xiao(肖仕奇)[1,2,3], Huiliang Chen(陈辉亮)[1,2,3], Weiya Zhou(周维亚)[1,2,3,†], and Sishen Xie(解思深)[1,2,3,‡]

[1] *Beijing National Laboratory for Condensed Matter Physics, Institute of Physics, Chinese Academy of Sciences, Beijing* 100190, *China*
[2] *Beijing Key Laboratory for Advanced Functional Materials and Structure Research, Beijing* 100190, *China*
[3] *University of Chinese Academy of Sciences, Beijing* 100049, *China*

(Received 14 April 2017; published online 6 June 2017)

Bridged strips consisting of carbon nanotubes and poly(vinylidene fluoride) are developed, which exhibit notable deflection in response to very low driven voltages (< 1 V), because of both the excellent conductivity of the unique carbon nanotube film and the powerful thermal expansion capability of the polymer. The actuators demonstrate periodic vibrations motivated by the alternating signals. The amplitude of displacement is dependent not only on the driven voltage but also on the applied frequency. The mechanism of actuation is confirmed to be the thermal power induced by the electrical heating. By accelerating the dissipation of heat, the vibration response at higher frequencies can be significantly enhanced. The useful locomotion shows great promise in potential applications such as miniature smart devices and micro power generators.

Keywords: carbon nanotube, poly(vinylidene fluoride), actuator, thermal expansion

PACS: 81.05.U–, 88.30.rh, 88.30.mj, 84.50.+d **DOI:** 10.1088/1674-1056/26/7/078101

1. Introduction

Actuators are devices that can offer displacement or mechanical output in response to various external stimuli (electricity, light, temperature, humidity, solvent, ions, etc.). The actuation phenomena or mechanisms are widely exhibited in nature as well as in the real-world applications, for which, pine cones,[1] wheat awns[2] and electrical motors are familiar examples. Carbon nanotubes (CNTs), because of their unique quasi-one-dimensional structure and outstanding properties in multiple aspects, such as high mechanical strength,[3,4] great optical absorbance,[5] superior electrical[6] and thermal[7,8] conductivities, have provided excellent platforms for the development of new types of actuators with improved performance.

Although CNTs have been adopted to build the molecular-scale rotational actuators[9] and oscillators,[10] their macroscopic assemblies in the form of fibres[11–14] or films,[15–20] in a practical sense, are probably more convenient to manipulate and utilize. Both the torsional motors made of CNT fibres[21–30] and the bending actuators which include CNT networks[31–40] have been extensively studied in the past few decades.

For the latter case, the composites, which consist of the polymer matrix and CNT reinforcement, are common structures that show enormous deflection driven by electricity[32,34,38] or light,[36,39] mainly due to the great efficiency of heat generation and transportation for CNTs and relatively large coefficient of thermal expansion (CTE) for polymers. Therefore, the choice of the matrix material and the distribution of CNTs in it are critical to the performance for this kind of actuator.

As is well known, the uniform dispersion of CNTs in the polymer precursor is a very difficult task. In order to achieve the desired electrical conductivity, a larger amount of CNTs should be added to form the interconnected conductive network,[32,34] which means consuming much longer time for the mixing treatment. With respect to the polymer, polydimethylsiloxane (PDMS)[34,38,41,42] is frequently selected as a result of its prominent CTE, which is as large as[39] 310×10^{-6} K^{-1} and more favourable to the remarkable deflection. Nevertheless, due to the extreme softness and poor modulus (0.7–0.9 MPa, 20–100 °C)[39] of PDMS, the stress output may not be satisfactory, especially on some force-demand occasions. In addition, most works have focused on the bending movement by a cantilever configuration,[35–39] i.e., with one-end tethered and the other end free. The bridge configuration[32,34] in which both ends are fixed has been rarely investigated.

To solve those problems, in this work we fabricated triple-layer composites, through combining unique CNT films of continuous reticulation, with poly(vinylidene fluoride) (PVDF), which has not only relatively large CTE (127×10^{-6} K^{-1}) but also significant modulus (8.3 GPa, 20–100 °C).[39,43] With a bridge configuration, the as-prepared

*Project supported by the National Basic Research Program of China (Grant No. 2012CB932302), the National Natural Science Foundation of China (Grant Nos. 11634014, 51172271, and 51372269), and the "Strategic Priority Research Program" of the Chinese Academy of Sciences (Grant No. XDA09040202).

†Corresponding author. E-mail: wyzhou@iphy.ac.cn
‡Corresponding author. E-mail: ssxie@iphy.ac.cn

© 2017 Chinese Physical Society and IOP Publishing Ltd

actuators demonstrated impressive displacement and considerable stress output by exerting very low voltages.

2. Results and discussion

The CNT film, as illustrated in Fig. 1(a), was obtained by stacking thin films which were directly and continuously synthesized via the float-catalyst chemical vapour deposition (FCCVD) method.[44] Due to the greater length of the tubes and vigorous inter-tube or inter-buddle entanglement (Fig. 1(b)), the electrical conductivity attains up to $\sim 2 \times 10^3$ S/cm and the tensile strength reaches as large as ~ 450 MPa.[17,44] The buckypapers,[15,20] prepared by the solution-based vacuum filtration method, in contrast, are much less conductive and robust, because of the short tube length and weak junctions between tubes. Moreover, another advantage of the CNT networks is their ability to carry out conformal and reversible deformation with the polymer layer.[19] As displayed by the *I–V* curve in Fig. 1(d), the resistance of the CNT strip (Dimensions: 20 mm×2 mm×1.6 μm) was 31.5 Ω, and that of its composite with PVDF in the same dimension slightly increased to 34.6 Ω, which is still one order of magnitude more conductive than the RGO/PVDF counterpart (20 mm×3 mm, the thickness of the RGO layer is 3–4 μm).[43] Therefore, these superior characteristics of our CNT films will significantly facilitate the realization of stable actuation at low driven voltages.

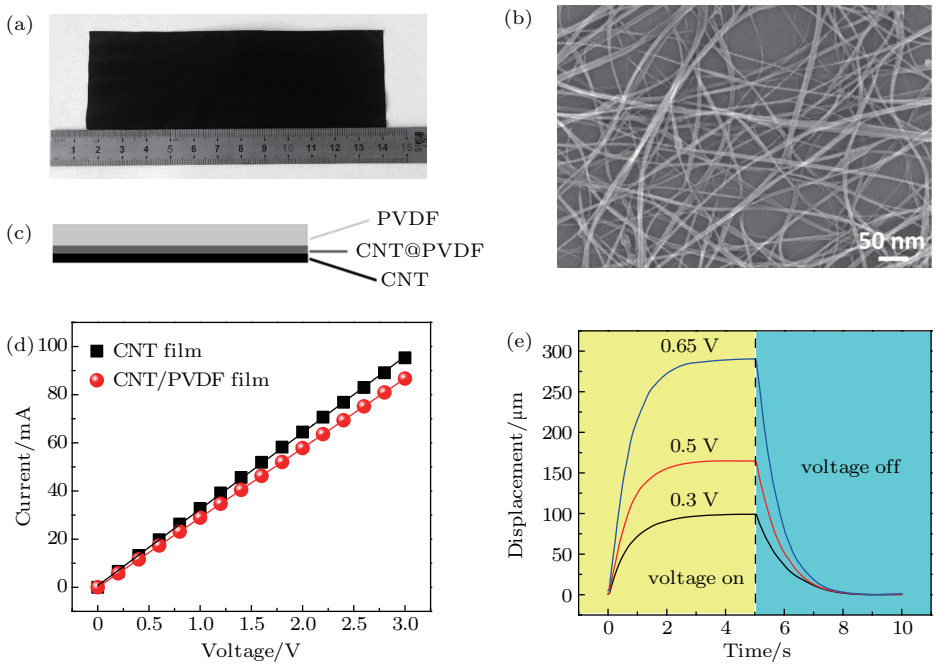


Fig. 1. (color online) (a) Optical photograph of the stacked CNT film. (b) Scanning electron micrograph of the directly synthesized CNT film. (c) The triple-layer structure of the CNT/PVDF composite film. (d) DC current–voltage (*I–V*) curve of the stacked CNT film (dimensions: 20 mm×2 mm×1.6 μm) and CNT/PVDF composite film (dimensions: 20 mm×2 mm×31.3 μm). For both, the correlation factor *R* of the linear fitting is more than 0.9998. (e) Time evolution of the displacement at different DC driven voltages for the composite film in panel (d). The voltages are eliminated after 5 s.

The details of the preparation of the CNT/PVDF composite films are shown in the experimental section. Interestingly, by measuring the resistance along the bottom and top face, we found that the as-prepared film should be divided into three parts, namely, PVDF, CNT@PVDF and CNT layer (Fig. 1(c)), because one side was probed insulating and the other side showed great conductivity. This feature suggested the PVDF precursor could not totally penetrate through the CNT network, probably due to the more dense packing and much larger depth of the stacked CNT film (Fig. 1(a)). Nevertheless, as a result of the exposed CNT layer, better electrical contact between the composite sample and the electrode could be anticipated. Typically, as depicted in Fig. 2, a strip with 2 mm in width and 25 mm in length was cut from the as-prepared hybrid film, and suspended between two bulged stages on the glass substrate, with a distance of 20 mm. Subsequently, silver paste was used to anchor the two ends of the strip onto the bulges and also served as the electrodes. In addition, a laser displacement sensor, which was set up right over the middle part of the strip, was introduced to track and record the actuation displacement. Once applied with a low DC voltage of less than 1 V, although much smaller than the previously reported values for CNT/Chitosan[32] (5 V) and CNT/PDMS[34] (30 V) hybrid films, the shape of our composite strip immediately transformed from a line (Fig. 2(c)) to a notable arc (Fig. 2(d)). The reverse process happened when the voltage was attenuated. The strip produced much larger displacement (curvature) at a faster rate with a higher driven voltage and could recover to the initial state (Fig. 1(e)). In general, the reversible actuation was kept with the applied voltage no more than 0.7 V (for 5 s), beyond which permanent rheological deformation was turned on, due to the excessive thermal power that caused rapid heat accumulation.

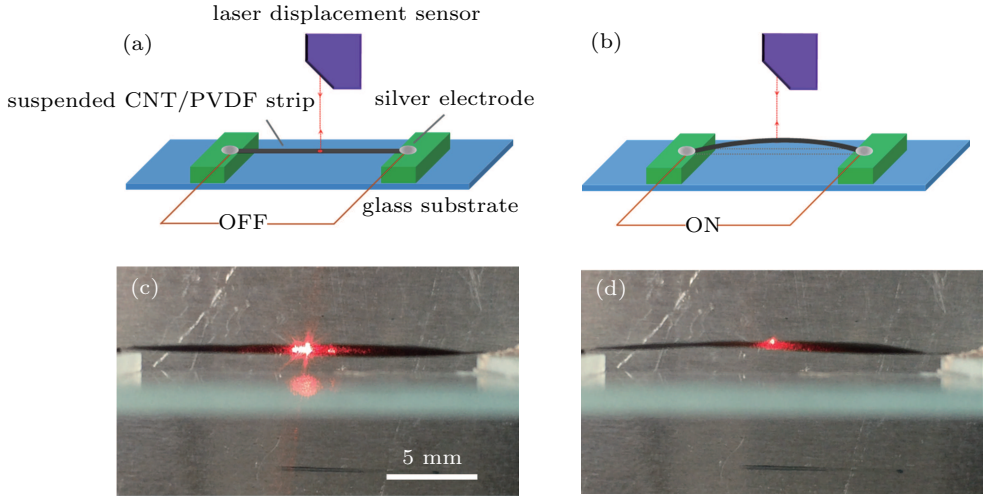


Fig. 2. (color online) (a), (b) Schematic illustration of the experimental design for the actuation. The CNT/PVDF composite strip is suspended between two bulged stages on the glass substrate. A laser displacement sensor is placed perpendicularly above the middle part of the strip to measure the actuation. (c), (d) Optical photograph of the CNT/PVDF composite strip (c) before and (d) after actuation. The driven voltage in panel (d) is 0.65 V and the displacement is $\sim$ 290 μm.

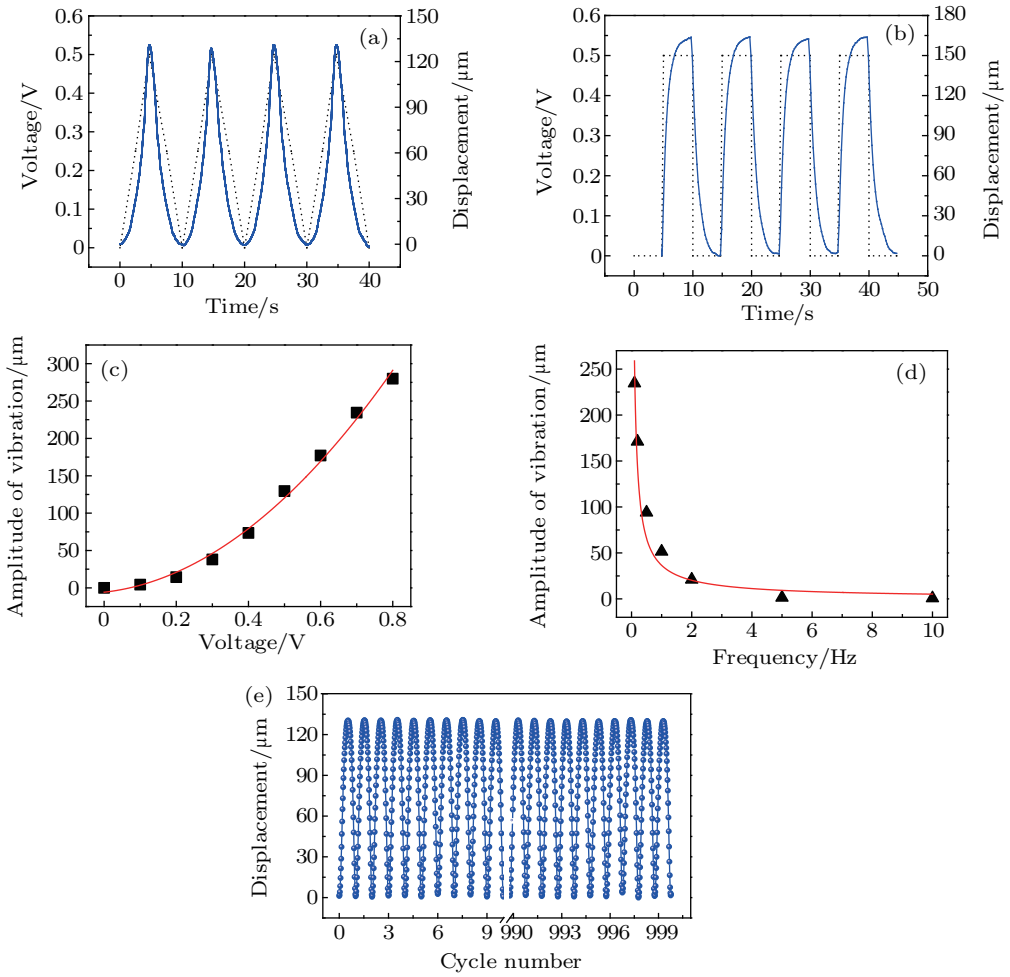


Fig. 3. (color online) Actuation displacement driven by (a) triangle wave voltage and (b) square wave voltage, both of 0–0.5 V and 0.1 Hz. Displacement amplitude dependence on the (c) voltage and (d) frequency. The red lines demonstrate the fitting to the experimental data. The Adj. *R*-Square values are (c) 0.9922 and (d) 0.9402, respectively. Both driven signals are triangle wave voltage. The frequency in panel (c) is 0.1 Hz, and the voltage in panel (d) is 0–0.7 V. (e) Cycle test of the actuation performance. The actuation is driven by continuously applying a triangle wave voltage of 0–0.5 V and 0.1 Hz.

Besides the above features, driven by alternating voltages, the CNT/PVDF composite films can generate periodic vibration, as shown by Videos 1 and 2, and Figs. 3(a) and 3(b), which indicates the electrical response is triggered by signals with different amplitudes and waveforms. The displacement coherently changed with the driven voltage, but some notable

relaxation came out characteristic of the slow heat dissipation in the case of square waves. Figure 3(c) exhibits the dependence of the vibrational feedback on the actuating voltage, with the increase of which, the amplitude was parabolically enhanced, just in coincidence with the correlation between the electrical heating power and the applied DC voltage. At a certain voltage amplitude (Fig. 3(d)), the lower the applied frequency, the larger the resulted displacement, because more heat was provided in each period. At larger frequencies, the actuation showed a sharp decay which was approximately in inverse proportion to the applied frequency and nearly vanished at about 10 Hz. This means the breath-like vibration is more suitable to be used on some specific occasions, where stable, reversible and large deformation or stress output of not high-speed rhythm is required.

To the thermally driven polymer-based actuators,[32,35–38,43] the limitation of relatively low working frequency is ubiquitous, for both bridge and cantilever configurations, which is determined by the actuation mechanism as well as the inherent physical properties of the chosen material. The reason may partly lie on the notable viscoelasticity of polymers at higher temperatures, but mainly, the phenomenon is due to the slow rate of heat dissipation on general conditions. Therefore, although a great quantity of heat is instantaneously generated in virtue of the boosted electrical power, that heat can hardly be dissipated at the same short period, which makes large actuation at more rapid frequency extremely difficult to realize. As illustrated in Fig. 4(a), driven by a triangle wave voltage of 0–1.4 V and 5 Hz for 20 cycles, the sample initially showed a large and fast deformation, which then slowly rose in a wave form with a vibration amplitude of $\sim$ 28 μm.

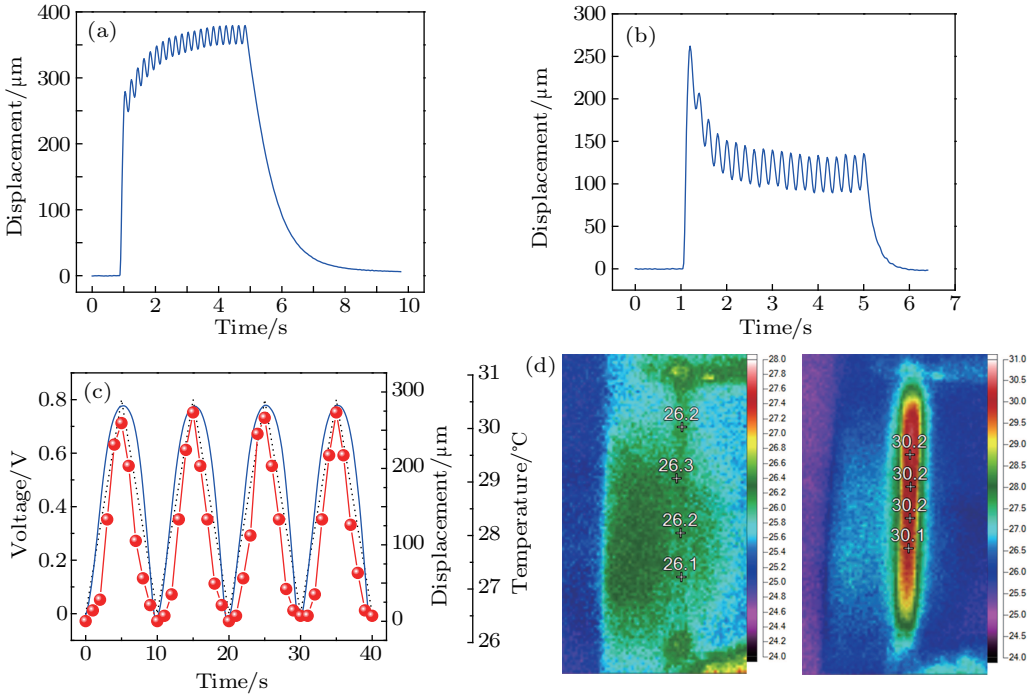


Fig. 4. (color online) (a), (b) Time evolution of the actuation displacement. The actuation is driven by a triangle wave voltage of 0–1.4 V and 5 Hz for 20 cycles. In panel (a), the heat dissipation of the sample is in natural conditions. While in panel (b), an electrical fan is intentionally exploited to assist the heat dissipation. (c) Displacement and temperature change driven by a triangle voltage of 0–0.8 V and 0.1 Hz. (d) Thermal image of the sample in panel (c) at the (left) minimum and (right) maximum temperature and deformation.

Under some particular circumstances, however, the vibration at higher frequencies may be promoted. In the control experiment, we adopted a small electrical fan to intentionally accelerate the heat dissipation, by which, the amplitude was effectively improved to $\sim$ 40 μm (Fig. 4(b)), compared with that on natural conditions (Fig. 4(a)). This was because the wind-blow of the fan had induced forced convection, which, in the sense of taking heat away, was more efficient than through the pure conduction and free convection. The wind effect was also reflected by the immediate drop from the initial large displacement and much quicker fading after the voltage was off.

The temperature variation of the composite film had also been monitored in real time, along with the mechanical response. As displayed in Fig. 4(c), the temperature change kept pace with the displacement, and both of them were accompanied in the same rhythm by the driven voltage, which hinted the close relation between the electrical heating and the actuation. To illustrate the thermal actuation mechanism, we calculated the resulted deformation on the basis of two perspectives (see details of the calculation scheme in the experimental section). On one hand, from the point of view of temperature change, the quantity of which was $\sim$ 4 K as shown in

Figs. 4(c) and 4(d) and Video 4, the strain contributed by the heat was estimated as $\sim 5.08 \times 10^{-4}$. On the other hand, the geometrical analysis of this corresponding case revealed that the total strain should be $\sim 5.21 \times 10^{-4}$. The remarkable consistence between the two results perfectly confirmed that the exhibited actuation completely stemmed from the heat, which drove the effective expansion of the polymer to perform cooperative deformation with the CNT network.

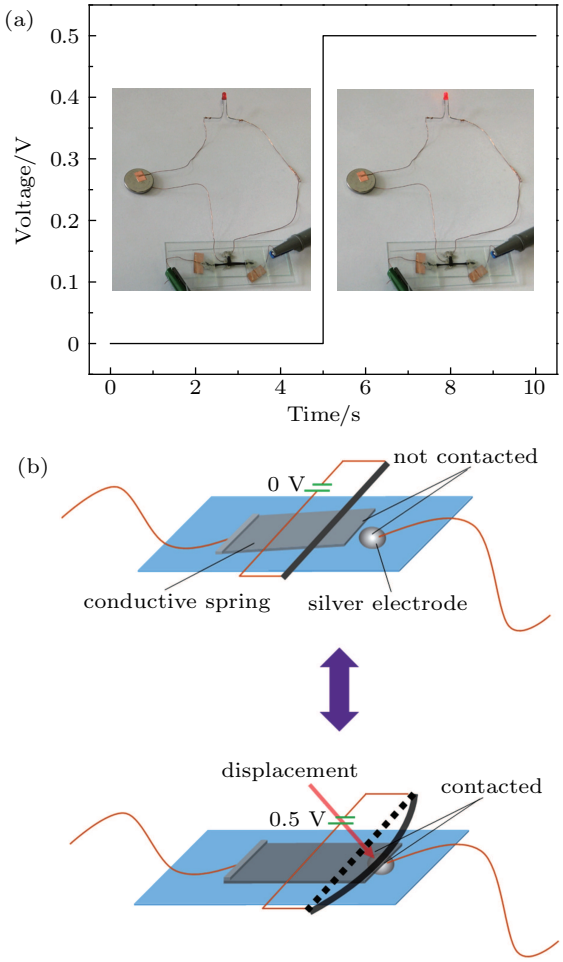


Fig. 5. (color online) (a) Switch application of the CNT/PVDF actuator. The LED can be triggered on through the actuation of the CNT/PVDF strip driven by a low voltage of 0.5 V. (b) Schematic illustration of the structure and mechanism for the part which is enclosed by the dark grey rectangle in panel (a). The actuation of the CNT/PVDF strip generates curvature and meanwhile exerts enough stress on the conductive "spring" to make it closely contacted with the bottom silver electrode.

To give an example, herein, we demonstrate the application of the bridged CNT/PVDF strip to act as a circuit switch. As illustrated in Fig. 5 and Video 3, the LED was immediately turned on with the fired strip curvature, the actuating voltage of which was as low as 0.5 V. The generated stress was estimated to be $\sim$ 1.5 MPa. As a result, the conductive "spring" (represented by the light grey part in Fig. 5(b), see details in the experimental section) was forced to approach and finally contacted with the electrode on the substrate, which thus connected the power supply.

3. Conclusion and perspectives

In summary, we have fabricated a triple-layer composite structure, which consists of both the directly synthesized CNT films, with high strength and superb conductivity, and the PVDF that is of considerable merit in CTE and Young's modulus. On the basis of a bridge configuration, they have exhibited notable actuation driven by very low voltages of less than 1 V. The source of the actuation energy is the thermal power from the electrical heating. By accelerating the rate of heat dissipation, the vibration amplitude at higher frequencies can be effectively improved. It is believed that these devices are promising in applications such as artificial muscles, miniature robots, and power generation.

4. Experimental

4.1. Preparation of the PVDF precursor

PVDF/N,N-Dimethylformamide (DMF) solution with a concentration of 100 mg/mL was prepared by adding 0.2 g PVDF powder (average Mw $\sim$ 534000 by GPC, purchased from Sigma-Aldrich) into 2 mL DMF solvent (AR, purchased from Sinopharm Chemical Reagent CO., Ltd.). To enhance the adhesion of PVDF with CNT, polyvinylpyrrolidone (PVP, GR, purchased from Sinopharm Chemical Reagent CO., Ltd.) in mass ratio of 1:20 with PVDF was also added. The mixture was then ultrasonically treated for 50 min to obtain the uniform precursor.

4.2. Preparation of the CNT/PVDF composite film

CNT film with a thickness of $\sim$ 1.6 μm was prepared by stacking the directly obtained thin film.[44] Subsequently, a 25 mm×25 mm square-shaped film was cut and spread out on a 20 mm×20 mm glass substrate. In aid of flattening the film and increasing its adhesion with the substrate, a few drops of ethanol were added. The PVDF precursor with a volume of 210 μL was added to the flattened film, and then heated in an oven with a temperature of 85 °C for 1 h. The cured composite film could be easily taken off the glass substrate.

4.3. Preparation of the switch structure

A Polyethylene terephthalate (PET) film (Dimensions: 20 mm×3 mm×180 μm) was cut and attached at one side with the stacked CNT film (1.6 μm in thickness). Subsequently, one end of the PET was fixed on the substrate by using the silver paste, with the other end left a very short distance from the silver electrode (as shown in Fig. 5(b)), which was right below the CNT side of the PET. The PET played the role of a conductive "spring". By imposing a force on the "spring", when the CNT film was in contact with the bottom electrode, the circuit was connected. If the force was eliminated, the "spring" recovered to the initial state and the circuit was cut off.

4.4. Characterization

SEM morphologies of the pristine CNT films were examined using a Hitachi S5200 SEM system operated at 5 kV. The driven voltage was imposed through a Zahner Im6 electrochemical workstation, choosing the PVI program in the Thales software package. A Keyence LK-H050 laser displacement sensor was utilized to track and record the displacement of the strip actuator. Thermal images were taken with a Fluke Ti25 infrared camera.

4.5. Calculation scheme of the strain and stress

As shown in Fig. 6, where l_0 and l' respectively denote the original and deformed length of the sample, d denotes the displacement of the middle part, and r is the radius of curvature, their geometrical relation can be expressed as

$$(r-d)^2+(l_0/2)^2=r^2.$$

From this equation, the radius of curvature r is readily obtained as

$$r=(l_0^2+4d^2)/8d.$$

Therefore, the curvature K is

$$K=8d/(l_0^2+4d^2).$$

In addition, the sample length after elongation can be represented as

$$l'=2r\arcsin(l_0/2r).$$

The total strain can thus be calculated as

$$\varepsilon_{\text{total}}=(l'-l_0)/l_0\times 100\%.$$

The contribution of the temperature increase ΔT to the strain is

$$\varepsilon_{\text{T}}=\alpha_{\text{T}}\Delta T,$$

where α_T is the coefficient of linear thermal expansion of PVDF.

If $\varepsilon_{\text{T}}\approx\varepsilon_{\text{total}}$, we can confirm that the actuation power totally comes from the electrical heating.

Finally, with the Young modulus of PVDF denoted as E, the generated stress σ is

$$\sigma=E\varepsilon_{\text{total}}.$$

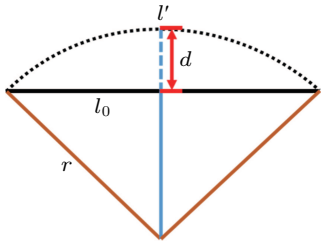


Fig. 6. (color online) Geometric modelling of the bridged CNT/PVDF actuators.

References

[1] Dawson J, Vincent J F V and Rocca A M 1997 *Nature* **390** 668
[2] Elbaum R, Zaltzman L, Burgert I and Fratzl P 2007 *Science* **316** 884
[3] Yu M F, Files B S, Arepalli S and Ruoff R S 2000 *Phys. Rev. Lett.* **84** 5552
[4] Peng B, Locascio M, Zapol P, Li S, Mielke S L, Schatz G C and Espinosa H D 2008 *Nat. Nanotech.* **3** 626
[5] Kataura H, Kumazawa Y, Maniwa Y, Umezu I, Suzuki S, Ohtsuka Y and Achiba Y 1999 *Synthetic Metals* **103** 2555
[6] Mann D, Javey A, Kong J, Wang Q and Dai H J 2003 *Nano Lett.* **3** 1541
[7] Pop E, Mann D, Wang Q, Goodson K E and Dai H J 2006 *Nano Lett.* **6** 96
[8] Fujii M, Zhang X, Xie H Q, Ago H, Takahashi K, Ikuta T, Abe H and Shimizu T 2005 *Phys. Rev. Lett.* **95** 065502
[9] Fennimore A M, Yuzvinsky T D, Han W Q, Fuhrer M S, Cumings J and Zettl A 2003 *Nature* **424** 408
[10] Sazonova V, Yaish Y, Ustunel H, Roundy D, Arias T A and McEuen P L 2004 *Nature* **431** 284
[11] Jiang K L, Li Q Q and Fan S S 2002 *Nature* **419** 801
[12] Koziol K, Vilatela J, Moisala A, Motta M, Cunniff P, Sennett M and Windle A 2007 *Science* **318** 1892
[13] Ma W, Liu L, Zhang Z, Yang R, Liu G, Zhang T, An X, Yi X, Ren Y, Niu Z, Li J, Dong H, Zhou W, Ajayan P M and Xie S 2009 *Nano Lett.* **9** 2855
[14] Behabtu N, Young C C, Tsentalovich D E, Kleinerman O, Wang X, Ma A W K, Bengio E A, ter Waarbeek R F, de Jong J J, Hoogerwerf R E, Fairchild S B, Ferguson J B, Maruyama B, Kono J, Talmon Y, Cohen Y, Otto M J and Pasquali M 2013 *Science* **339** 182
[15] Wu Z C, Chen Z H, Du X, Logan J M, Sippel J, Nikolou M, Kamaras K, Reynolds J R, Tanner D B, Hebard A F and Rinzler A G 2004 *Science* **305** 1273
[16] Song L, Ci L, Lv L, Zhou Z P, Yan X Q, Liu D F, Yuan H J, Gao Y, Wang J X, Liu L F, Zhao X W, Zhang Z X, Dou X Y, Zhou W Y, Wang G, Wang C Y and Xie S S 2004 *Adv. Mater.* **16** 1529
[17] Ma W, Song L, Yang R, Zhang T, Zhao Y, Sun L, Ren Y, Liu D, Liu L, Shen J, Zhang Z, Xiang Y, Zhou W and Xie S 2007 *Nano Lett.* **7** 2307
[18] Jiang K, Wang J, Li Q, Liu L, Liu C and Fan S 2011 *Advanced Materials* **23** 1154
[19] Li J, Gao Y, Ma W, Liu L, Zhang Z, Niu Z, Ren Y, Zhang X, Zeng Q, Dong H, Zhao D, Cai L, Zhou W and Xie S 2011 *Nanoscale* **3** 3731
[20] Blackburn J L, Barnes T M, Beard M C, Kim Y H, Tenent R C, McDonald T J, To B, Coutts T J and Heben M J 2008 *Acs Nano* **2** 1266
[21] Foroughi J, Spinks G M, Wallace G G, Oh J, Kozlov M E, Fang S, Mirfakhrai T, Madden J D W, Shin M K, Kim S J and Baughman R H 2011 *Science* **334** 494
[22] Lima M D, Li N, de Andrade M J, Fang S, Oh J, Spinks G M, Kozlov M E, Haines C S, Suh D, Foroughi J, Kim S J, Chen Y, Ware T, Shin M K, Machado L D, Fonseca A F, Madden J D W, Voit W E, Galvao D S and Baughman R H 2012 *Science* **338** 928
[23] Lee J A, Kim Y T, Spinks G M, Suh D, Lepro X, Lima M D, Baughman R H and Kim S J 2014 *Nano Lett.* **14** 2664
[24] Chun K Y, Hyeong Kim S, Kyoon Shin M, Hoon Kwon C, Park J, Tae Kim Y, Spinks G M, Lima M D, Haines C S, Baughman R H and Jeong Kim S 2014 *Nature Commun.* **5** 3322
[25] Lima M D, Hussain M W, Spinks G M, Naficy S, Hagenasr D, Bykova J S, Tolly D and Baughman R H 2015 *Small* **11** 3113
[26] Kwon C H, Chun K Y, Kim S H, Lee J H, Kim J H, Lima M D, Baughman R H and Kim S J 2015 *Nanoscale* **7** 2489
[27] Chen P, Xu Y, He S, Sun X, Pan S, Deng J, Chen D and Peng H 2015 *Nat. Nanotech.* **10** 1077
[28] He S, Chen P, Qiu L, Wang B, Sun X, Xu Y and Peng H 2015 *Angewandte Chemie* **54** 14880
[29] Gu X, Fan Q, Yang F, Cai L, Zhang N, Zhou W, Zhou W and Xie S 2016 *Nanoscale* **8** 17881
[30] Mirfakhrai T, Oh J, Kozlov M, Fok E C W, Zhang M, Fang S, Baughman R H and Madden J D W 2007 *Smart Materials and Structures* **16** S243
[31] Baughman R H, Cui C X, Zakhidov A A, Iqbal Z, Barisci J N, Spinks G M, Wallace G G, Mazzoldi A, De Rossi D, Rinzler A G, Jaschinski O, Roth S and Kertesz M 1999 *Science* **284** 1340
[32] Hu Y, Chen W, Lu L, Liu J and Chang C 2010 *Acs Nano* **4** 3498

[33] Li J, Ma W, Song L, Niu Z, Cai L, Zeng Q, Zhang X, Dong H, Zhao D, Zhou W and Xie S 2011 *Nano Lett.* **11** 4636
[34] Hu Y, Wang G, Tao X and Chen W 2011 *Macromolecular Chemistry and Physics* **212** 1671
[35] Chen L, Liu C, Liu K, Meng C, Hu C, Wang J and Fan S 2011 *Acs Nano* **5** 1588
[36] Zhang X, Yu Z, Wang C, Zarrouk D, Seo J W, Cheng J C, Buchan A D, Takei K, Zhao Y, Ager J W, Zhang J, Hettick M, Hersam M C, Pisano A P, Fearing R S and Javey A 2014 *Nat. Commun.* **5** 2983
[37] Li Q, Liu C, Lin Y H, Liu L, Jiang K and Fan S 2015 *Acs Nano* **9** 409
[38] Chen L, Weng M, Zhou Z, Zhou Y, Zhang L, Li J, Huang Z, Zhang W, Liu C and Fan S 2015 *Acs Nano* **9** 12189
[39] Tai Y, Lubineau G and Yang Z 2016 *Adv. Mater.* **28** 4665
[40] Chen L, Weng M, Zhang W, Zhou Z, Zhou Y, Xia D, Li J, Huang Z, Liu C and Fan S 2016 *Nanoscale* **8** 6877
[41] Taccola S, Greco F, Sinibaldi E, Mondini A, Mazzolai B and Mattoli V 2015 *Adv. Mater.* **27** 1668
[42] Li B, Du T, Yu B, van der Gucht J and Zhou F 2015 *Small* **11** 3494
[43] Xiao P, Yi N, Zhang T, Huang Y, Chang H, Yang Y, Zhou Y and Chen Y 2016 *Adv. Sci.* **3** 1500438
[44] Zhang Q, Li K, Fan Q, Xia X, Zhang N, Xiao Z, Zhou W, Yang F, Wang Y, Liu H and Zhou W 2017 *Chin. Phys. B* **26** 28802